Int. J. Heat Mass Transfer. Vol. 33, No. 9, pp. 1895–1908, 1990
Printed in Great Britain

0017-9310/90 $3.00 + 0.00

Stability of boiling in porous media

P. S. RAMESH and K. E. TORRANCE
Sibley School of Mechanical and Aerospace Engineering, Cornell University, Ithaca, NY 14853, U.S.A.

(*Received* 10 *May* 1989 *and in final form* 25 *October* 1989)

Abstract—The onset of two-dimensional roll convection in the presence of boiling is studied for a fluid-saturated horizontal porous layer. The layer is heated from below and cooled from above. The rest-state phase structure consists of a liquid region overlying a two-phase region. The two important parameters in the problem are the Rayleigh number in the liquid region (Ra) and the dimensionless heat flux at the bottom boundary (Q_b). Both liquid-dominated and vapor-dominated two-phase regions are investigated. For liquid-dominated systems, the convective instability is driven mainly by buoyancy in the liquid region, while for vapor-dominated systems the instability is driven by the gravitational instability of the overlying layers. For liquid-dominated systems, a stability diagram in Ra–Q_b parameter space is used to interpret prior laboratory experiments.

1. INTRODUCTION

HEAT TRANSFER in porous media is a subject of growing interest because of extensive engineering applications. Much of the existing literature deals with single-phase thermal convection. However, in many problems of interest such as geothermal energy or post accident scenarios in nuclear reactors, the porous medium consists of single-phase (liquid) as well as two-phase (liquid + vapor) regions. This paper analyzes the onset of thermal convection in a porous medium containing both single-phase and two-phase regions.

The phase structure in fluid-saturated porous media heated from below and cooled from above is layered after the onset of boiling, with a liquid region overlying a two-phase region, as sketched in Fig. 1. Laboratory

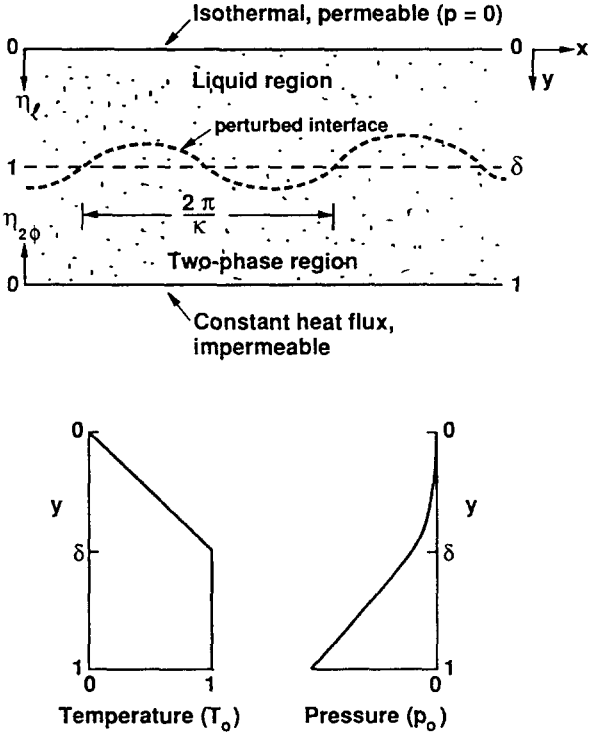

FIG. 1. Geometry of the porous layer, and temperature and pressure profiles of the basic state.

NOMENCLATURE

C	specific heat
$\mathbf{e}_x, \mathbf{e}_y$	unit vectors in x, y, respectively
g	acceleration due to gravity
h_{fg}	latent heat of vaporization
H	height of the porous medium
k_e	effective thermal conductivity of the porous medium
$k_{r\ell}, k_{rv}$	relative permeabilities for liquid and vapor, respectively
K	permeability of the porous medium
p	dimensionless pressure
q_b^*	heat flux at the bottom boundary
Q_b	dimensionless heat flux at the bottom boundary, $q_b^* H/(k_e(T_{sat}^* - T_0^*))$
Ra	Rayleigh number for the liquid phase, $(KHg\beta_\ell(T_{sat}^* - T_0^*))/(\nu_\ell \alpha_\ell)$
Ra_f	heat flux Rayleigh number for the liquid phase, $(Kq_b^* H^2 g\beta_\ell)/(k_e \nu_\ell \alpha_\ell)$
$Ra_{2\phi}$	Rayleigh number based on liquid–vapor density difference, $(KHg(1-\bar{\rho}_v))/(\nu_\ell \alpha_\ell)$
S	liquid saturation in the two-phase region
T	dimensionless temperature
T^*	temperature
T_0^*	temperature at the top boundary
T_{sat}^*	saturation temperature
u, v	dimensionless x and y components of velocity, respectively
$\mathbf{v}$	dimensionless velocity vector
x, y	horizontal and vertical coordinates, see Fig. 1.

Greek symbols

α_ℓ	liquid thermal diffusivity
α_1	function in equation (12)
α_2	function in equation (13)
β_ℓ	liquid thermal expansion coefficient
β_1	$((1-\phi)\rho_s C_s + \phi\rho_\ell C_\ell)/(\rho_\ell C_\ell)$
β_2	$\phi(1-\bar{\rho}_v)$
γ	density ratio parameter, $\beta_\ell(T_{sat}^* - T_0^*)/(1-\bar{\rho}_v)$
δ	interface position
Δ	amplitude of perturbation of the interface
η_ℓ	transformed vertical spatial coordinate in liquid region
$\eta_{2\phi}$	transformed vertical spatial coordinate in two-phase region
Θ	amplitude of temperature perturbation
κ	wave number of the perturbation
λ	latent heat parameter, $h_{fg}/(C_\ell(T_{sat}^* - T_0^*))$
μ	dynamic viscosity
$\bar{\mu}_\ell$	μ_ℓ/μ_v
ν	kinematic viscosity
ξ	transformed horizontal spatial coordinate
Π	amplitude of pressure perturbation
ρ	density
$\bar{\rho}_v$	ρ_v/ρ_ℓ
σ	growth rate of perturbation
τ	transformed time variable
ϕ	porosity of the porous medium
Ω	amplitude of v velocity perturbation.

Subscripts and superscripts

cr	critical state for the onset of convection
ℓ	liquid
s	porous material
v	vapor
0	basic state
1	perturbed state.

experiments [1–3] have shown that the liquid region temperature profile may be conductive or convective, whereas the two-phase region is essentially isothermal at the saturation temperature. The two-phase region may be liquid-dominated or vapor-dominated. Heat transport across the isothermal two-phase region occurs by vertical counterpercolation of liquid and vapor. Liquid evaporates on the heating surface and vapor condenses at the interface between the liquid and two-phase regions. Experiments have indicated that thermal convection in the liquid region may occur before the onset of boiling [3] as well as after the onset of boiling [2]. Visualization experiments [4] indicate that after the onset of convection, the liquid region streamlines penetrate the two-phase region, which implies considerable interaction between the two regions. However, no previous study has analyzed the onset of convection in porous media containing both single-phase and two-phase regions.

The problem of thermal convection in a porous medium with a liquid region overlying a two-phase region has some unique features. There are two mechanisms for instability: the first is buoyancy produced by density gradients arising from temperature variations in the liquid region. The second mechanism is gravitational instability due to the heavier liquid region overlying the lighter two-phase region. The gravitational instability differs from the classical gravitational instability of superposed fluids [5] because the interface between the liquid and two-phase regions is permeable, and therefore permits both heat and mass transfer across it. In a related study, Schubert and Straus [6] have considered the stability of a vapor-dominated geothermal system with a liquid region overlying a dry vapor region. They concluded that such systems are stable provided the permeability of the porous media is sufficiently low. The stabilization is provided by phase change processes

at the interface. When liquid penetrates the interface, the interface distorts to remain on the Clapeyron curve, resulting in an adverse pressure gradient. Schubert and Straus, however, did not consider the effects of buoyancy within the liquid or the effect of a possible liquid phase in the underlying steam zone.

In the present work, a linear stability analysis of boiling in a porous medium, heated from below and cooled from above, is carried out. The basic state is one-dimensional with a liquid region overlying a two-phase region, and the liquid region temperature profile is conductive. The two important parameters in the problem are the Rayleigh number (Ra) which accounts for buoyancy effects in the liquid region, and the dimensionless heat flux at the bottom boundary (Q_b) which controls the height of the two-phase region. As the height of the two-phase region tends to zero, the analysis reduces to the onset of convection in a single-phase region with an effective Rayleigh number given by $Ra\,Q_b$. We consider both liquid-dominated and vapor-dominated two-phase regions. For liquid-dominated systems, we show that the critical Rayleigh number is lowered by the presence of the two-phase region. We present a stability diagram in the Ra–Q_b parameter space and use it to interpret laboratory experiments. For vapor-dominated systems, at sufficiently low liquid saturations, we show that instability is possible even in the absence of thermal buoyancy effects ($Ra = 0$), and compare our results with Schubert and Straus [6].

2. GOVERNING EQUATIONS

We consider a porous domain bounded by two horizontal parallel plates which are separated by a distance H. We assume the porous medium to be uniform, isotropic and fully saturated with fluid. The porous medium is heated from below and cooled from above. The phase structure after the onset of boiling consists of a liquid region overlying a two-phase region (see Fig. 1). Two-dimensional motion in the x–y plane is assumed. A complete discussion of the equations in the liquid and two-phase regions is given in ref. [7]. The Boussinesq approximation is used to account for buoyancy effects in the liquid region. The two-phase region is taken to be isothermal at the boiling temperature (T^*_{sat}).

The equations are made nondimensional using the following reference quantities: length, H; time, H^2/α_s (diffusion time scale); and temperature, $T = (T^* - T^*_0)/(T^*_{sat} - T^*_0)$ where T^*_0 is the temperature of the top boundary. The governing equations in the liquid and two-phase regions in dimensionless form are:

liquid

$$\nabla \cdot \mathbf{v}_\ell = 0 \quad \text{(continuity)} \tag{1}$$

$$\mathbf{v}_\ell = -\nabla p - Ra\,T\mathbf{e}_y \quad \text{(Darcy's equation)} \tag{2}$$

$$\beta_1 \frac{\partial T}{\partial t} + \mathbf{v}_\ell \cdot \nabla T = \nabla^2 T \quad \text{(energy)}; \tag{3}$$

two-phase

$$\beta_2 \frac{\partial S}{\partial t} + \nabla \cdot (\mathbf{v}_\ell + \bar{\rho}_v \mathbf{v}_v) = 0 \quad \text{(continuity)} \tag{4}$$

$$\mathbf{v}_\ell = -k_{r\ell}(\nabla p + Ra\,\mathbf{e}_y) \quad \text{(Darcy's equation for liquid)} \tag{5}$$

$$\mathbf{v}_v = -k_{rv}\bar{\mu}_\ell(\nabla p + Ra_{2\phi}\,\mathbf{e}_y) \quad \text{(Darcy's equation for vapor)} \tag{6}$$

$$\phi\bar{\rho}_v\lambda\frac{\partial}{\partial t}(1-S) + \nabla \cdot (\bar{\rho}_v\lambda\mathbf{v}_v) = 0 \quad \text{(energy)} \tag{7}$$

where T and p are the temperature and pressure respectively; $\mathbf{v}$ the velocity vector; and S the liquid saturation in the two-phase region. ϕ is the porosity of the porous medium; Ra the Rayleigh number in the liquid region which is based on the temperature difference $(T^*_{sat} - T^*_0)$; $Ra_{2\phi}$ the Rayleigh number in the two-phase region which involves the density difference between the phases. $\bar{\rho}_v$ is the ratio of vapor and liquid densities and λ is a latent heat parameter. β_1 and β_2 are constants involving the heat capacities and densities of liquid, vapor, and porous medium. $\bar{\mu}_\ell$ is the ratio of liquid and vapor dynamic viscosities. $\mathbf{e}_y$ is the unit vector in y which is assumed positive in the direction of the gravity vector. $k_{r\ell}$ and k_{rv} are the relative permeabilities for the liquid and vapor phases, respectively, which are typically functions of S. The subscripts ℓ, v, and s represent liquid, vapor, and porous medium, respectively.

The two Rayleigh numbers are related by a density ratio parameter, γ, given by

$$\gamma = \frac{Ra}{Ra_{2\phi}} = \frac{\beta_\ell(T^*_{sat} - T^*_0)}{1 - \bar{\rho}_v}.$$

γ is the ratio of the maximum density change in the liquid region to the density difference between phases in

the two-phase region. γ involves physical properties and boundary temperatures. If these are known, Ra and $Ra_{2\phi}$ are not independent, but are related by $Ra = Ra_{2\phi}\gamma$.

Note in equations (5) and (6), that the liquid and vapor phases in the two-phase region are locally taken to be at the same pressure, p. This follows when the mean radius of curvature of the interfaces separating the phases (at the pore level) is large, and the capillary pressure difference may be neglected. Thus, in equations (5) and (6), the flow of each phase is driven by the difference between ∇p and the hydrostatic gradient for the phase. Capillary pressure effects can arise for very fine grain porous media, or when wicking action (and not gravity) is important for the movement of the liquid phase. For simplicity, capillary pressure effects will be neglected in the present analysis.

The boundary conditions are:

$$\text{at} \quad y = 0: \quad T = 0, \quad p = 0 \quad \text{(isothermal, permeable)} \tag{8}$$

$$\text{at} \quad y = 1: \quad -\tilde{\rho}_v \lambda v_v = Q_b \quad \text{(constant heat flux)}$$

$$v_\ell + \tilde{\rho}_v v_v = 0 \quad \text{(impermeable)} \tag{9}$$

where v is the y velocity component, and Q_b the non-dimensional heat flux at the bottom. Note that Q_b is made dimensionless with $k_e(T^*_{sat} - T^*_0)/H$, which represents the maximum conduction flux across a liquid-saturated porous layer before the onset of boiling.

The interface between the liquid and two-phase regions is represented functionally by $y = \delta(x, t)$. The following compatibility conditions are prescribed at the interface:

$$p^+ = p^- \quad \text{(pressure is continuous across the interface)} \tag{10}$$

$$T^- = 1 \quad \text{(interface is at the phase change temperature)} \tag{11}$$

$$(\mathbf{v}_\ell^- - (\mathbf{v}_\ell^+ \tilde{\rho}_v \mathbf{v}_v^+) - \alpha_1 \mathbf{v}_i) \cdot \mathbf{n} = 0 \quad \text{(mass balance)} \tag{12}$$

$$(\nabla T^- + \tilde{\rho}_v \lambda \mathbf{v}_v^+ - \alpha_2 \mathbf{v}_i) \cdot \mathbf{n} = 0 \quad \text{(energy balance)} \tag{13}$$

where α_1, α_2 are functions of S given by $\alpha_1 = \phi(1-\tilde{\rho}_v)(1-S)$ and $\alpha_2 = \phi\tilde{\rho}_v\lambda(1-S)$. $\mathbf{v}_i$ is the local velocity of the interface, and $\mathbf{n}$ the unit vector normal to the interface. The superscripts $-$ and $+$ represent the liquid and the vapor sides of the interface, respectively. Note that capillary effects at the interface are neglected in equation (10), consistent with their neglect within the two-phase region.

It is more convenient to apply the compatibility conditions at the perturbed interface if the equations are transformed from the (t, x, y) space to (τ, ξ, η) space where $\tau = t$, $\xi = x$, and $\eta_\ell = y/\delta(x, t)$ (in liquid) or $\eta_{2\phi} = (1-y)/(1-\delta(x, t))$ (in two-phase).

Then

$$\nabla = \begin{cases} \left(\dfrac{\partial}{\partial\xi} - \dfrac{\eta_\ell}{\delta}\dfrac{\partial\delta}{\partial\xi}\dfrac{\partial}{\partial\eta_\ell}\right)\mathbf{e}_x + \dfrac{1}{\delta}\dfrac{\partial}{\partial\eta_\ell}\mathbf{e}_y & \text{(in liquid)} \\ \left(\dfrac{\partial}{\partial\xi} + \dfrac{\eta_{2\phi}}{1-\delta}\dfrac{\partial\delta}{\partial\xi}\dfrac{\partial}{\partial\eta_{2\phi}}\right)\mathbf{e}_x - \dfrac{1}{1-\delta}\dfrac{\partial}{\partial\eta_{2\phi}}\mathbf{e}_y & \text{(in two-phase)} \end{cases}$$

$$\nabla^2 = \begin{cases} \dfrac{\partial^2}{\partial\xi^2} - \left(\dfrac{\eta_\ell}{\delta}\dfrac{\partial^2\delta}{\partial\xi^2} - \dfrac{2\eta_\ell}{\delta^2}\left(\dfrac{\partial\delta}{\partial\xi}\right)^2\right)\dfrac{\partial}{\partial\eta_\ell} - \dfrac{2\eta_\ell}{\delta}\dfrac{\partial\delta}{\partial\xi}\dfrac{\partial^2}{\partial\xi\,\partial\eta_\ell} \\ \quad + \left(\left(\dfrac{\eta_\ell}{\delta}\right)^2\left(\dfrac{\partial\delta}{\partial\xi}\right)^2 + \dfrac{1}{\delta^2}\right)\dfrac{\partial^2}{\partial\eta_\ell^2} & \text{(in liquid)} \\ \dfrac{\partial^2}{\partial\xi^2} + \left(\dfrac{\eta_{2\phi}}{1-\delta}\dfrac{\partial^2\delta}{\partial\xi^2} + \dfrac{2\eta_{2\phi}}{(1-\delta)^2}\left(\dfrac{\partial\delta}{\partial\xi}\right)^2\right)\dfrac{\partial}{\partial\eta_{2\phi}} + \dfrac{2\eta_{2\phi}}{1-\delta}\dfrac{\partial\delta}{\partial\xi}\dfrac{\partial^2}{\partial\xi\,\partial\eta_{2\phi}} \\ \quad + \left(\left(\dfrac{\eta_{2\phi}}{1-\delta}\right)^2\left(\dfrac{\partial\delta}{\partial\xi}\right)^2 + \dfrac{1}{(1-\delta)^2}\right)\dfrac{\partial^2}{\partial\eta_{2\phi}^2} & \text{(in two-phase)} \end{cases}$$

$$\frac{\partial}{\partial t} = \begin{cases} \dfrac{\partial}{\partial\tau} - \dfrac{\eta_\ell}{\delta}\dfrac{\partial\delta}{\partial\tau}\dfrac{\partial}{\partial\eta_\ell} & \text{(in liquid)} \\ \dfrac{\partial}{\partial\tau} + \dfrac{\eta_{2\phi}}{1-\delta}\dfrac{\partial\delta}{\partial\tau}\dfrac{\partial}{\partial\eta_{2\phi}} & \text{(in two-phase).} \end{cases}$$

In summary, the dependent variables appearing in governing equations (1)–(13) are $\mathbf{v}_\ell$, $\mathbf{v}_v$, p, T, S and δ. In addition, functional relations for $k_{r\ell}$ and k_{rv} are required. Several dimensionless parameters involving physical

properties appear in the equations; namely, ϕ, $\tilde{\rho}_v$, $\tilde{\mu}_\ell$, $\rho_s C_s/\rho_\ell C_\ell$ (which appears in β_1), γ and λ. Although γ and λ involve the temperature difference $(T^*_{sat} - T^*_0)$, it will be convenient to regard them primarily as physical property parameters. In addition, two independent parameters appear, Ra and Q_b. This is in contrast to the single-phase convection problem which is governed by a single parameter Ra_f, the heat flux Rayleigh number. The additional parameter in the present set of equations, Q_b, is required to specify the two-phase region and the position of the phase change interface. Clearly, as the thickness of the two-phase region approaches zero, the two layer stability problem reduces to the single-phase convection problem with $Ra_f = Ra\, Q_b$.

3. LINEAR STABILITY ANALYSIS

3.1. *Basic state*

The basic state is one-dimensional as sketched in Fig. 1. The liquid region is motionless and heat is transferred therein by conduction alone. Heat is transferred across the two-phase region by the vertical counterpercolation of liquid and vapor. The basic state solution is given below.

Liquid

$$T_0 = \eta_\ell, \quad \frac{dp_0}{d\eta_\ell} = -Ra\,\eta_\ell \delta_0. \tag{14}$$

The rest position of the interface is given by $\delta_0 = 1/Q_b$.

Two-phase

$$v_{v,0} = -\frac{Q_b}{\tilde{\rho}_v \lambda}, \quad v_{\ell,0} = \frac{Q_b}{\lambda}$$

$$\frac{dp_0}{d\eta_{2\phi}} = (1-\delta_0)\frac{v_{\ell,0}}{k_{r\ell}} + (1-\delta_0)\,Ra. \tag{15}$$

Saturation S_0 is found from the following equation:

$$\frac{Q_b}{\lambda(Ra_{2\phi} - Ra)}\left(\frac{1}{k_{r\ell}} + \frac{1}{\tilde{\mu}_\ell \tilde{\rho}_v}\frac{1}{k_{rv}}\right) = 1. \tag{16}$$

We assume linear relative permeabilities, i.e. $k_{r\ell} = S$, and $k_{rv} = 1 - S$. Thus, equation (16) is quadratic and yields two solution branches for S_0: a liquid-dominated branch and a vapor-dominated branch (see Fig. 2). We consider both branches of saturation in our analysis. Note that there is also a maximum value of heat flux in Fig. 2 beyond which two-phase solutions do not exist [1]. Surpassing this limit implies dryout of the liquid phase in the two-phase region.

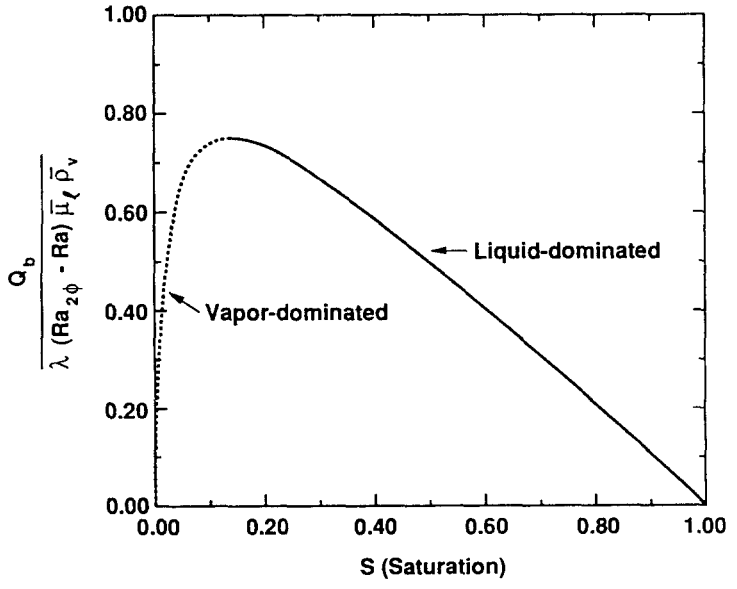

FIG. 2. Q_b saturation in the two-phase region of the basic state.

3.2. *Perturbed state*

We consider small perturbations about the basic state, and neglect second- and higher order terms. For example, $T = T_0 + \varepsilon T_1$, etc., where ε is small. The perturbation equations in τ, ξ, η coordinates are:

liquid

$$\frac{\partial u_{\ell,1}}{\partial \xi} + \frac{1}{\delta_0}\frac{\partial v_{\ell,1}}{\partial \eta_\ell} = 0$$

$$u_{\ell,1} = -\frac{\partial p_1}{\partial \xi} + \frac{\eta_\ell}{\delta_0}\frac{\mathrm{d}p_0}{\mathrm{d}\eta_\ell}\frac{\partial \delta_1}{\partial \xi}$$

$$v_{\ell,1} = -\frac{1}{\delta_0}\frac{\partial p_1}{\partial \eta_\ell} + \frac{1}{\delta_0^2}\frac{\mathrm{d}p_0}{\mathrm{d}\eta_\ell}\delta_1 - Ra\,T_1$$

$$\beta_1\frac{\partial T_1}{\partial \tau} - \beta_1\frac{\eta_\ell}{\delta_0}\frac{\mathrm{d}T_0}{\mathrm{d}\eta_\ell}\frac{\partial \delta_1}{\partial \tau} + \frac{1}{\delta_0}\frac{\mathrm{d}T_0}{\mathrm{d}\eta_\ell}v_{\ell,1} = \frac{\partial^2 T_1}{\partial \xi^2} - \frac{\eta_\ell}{\delta_0}\frac{\mathrm{d}T_0}{\mathrm{d}\eta_\ell}\frac{\partial^2 \delta_1}{\partial \xi^2} + \frac{1}{\delta_0^2}\frac{\partial^2 T_1}{\partial \eta_\ell^2}; \tag{17}$$

two-phase

$$\frac{\partial u_{\ell,1}}{\partial \xi} - \frac{1}{1-\delta_0}\frac{\partial v_{\ell,1}}{\partial \eta_{2\phi}} = -\phi\frac{\partial S_1}{\partial \tau}$$

$$u_{\ell,1} = -k_{r\ell}\frac{\partial p_1}{\partial \xi} - k_{r\ell}\frac{\eta_{2\phi}}{1-\delta_0}\frac{\mathrm{d}p_0}{\mathrm{d}\eta_{2\phi}}\frac{\partial \delta_1}{\partial \xi}$$

$$v_{\ell,1} = \frac{k_{r\ell}}{1-\delta_0}\frac{\partial p_1}{\partial \eta_{2\phi}} + \frac{k_{r\ell}}{(1-\delta_0)^2}\frac{\mathrm{d}p_0}{\mathrm{d}\eta_{2\phi}}\delta_1 + \frac{\dot{k}_{r\ell}}{1-\delta_0}\frac{\mathrm{d}p_0}{\mathrm{d}\eta_{2\phi}}S_1 - \dot{k}_{r\ell}\,Ra\,S_1$$

$$u_{v,1} = \tilde{\mu}_\ell\left(-k_{rv}\frac{\partial p_1}{\partial \xi} - k_{rv}\frac{\eta_{2\phi}}{1-\delta_0}\frac{\mathrm{d}p_0}{\mathrm{d}\eta_{2\phi}}\frac{\partial \delta_1}{\partial \xi}\right)$$

$$v_{v,1} = \tilde{\mu}_\ell\left(\frac{k_{rv}}{1-\delta_0}\frac{\partial p_1}{\partial \eta_{2\phi}} + \frac{k_{rv}}{(1-\delta_0)^2}\frac{\mathrm{d}p_0}{\mathrm{d}\eta_{2\phi}}\delta_1 + \frac{\dot{k}_{rv}}{1-\delta_0}\frac{\mathrm{d}p_0}{\mathrm{d}\eta_{2\phi}}S_1 - \dot{k}_{rv}\,Ra_{2\phi}\,S_1\right)$$

$$\frac{\partial u_{v,1}}{\partial \xi} - \frac{1}{1-\delta_0}\frac{\partial v_{v,1}}{\partial \eta_{2\phi}} = \phi\frac{\partial S_1}{\partial \tau} \tag{18}$$

where $\dot{k}_{r\ell,v} = \mathrm{d}k_{r\ell,v}/\mathrm{d}S$. For linear relative permeabilities, $\dot{k}_{r\ell} = 1$ and $\dot{k}_{rv} = -1$. The basic state variables are represented by the subscript 0 and the perturbed variables by the subscript 1. Note that the continuity and energy equations in equation (18) have been cast in a form different from that in equations (4) and (7).

A normal mode expansion is used for the perturbation variables, i.e. $T_1 = \Theta(\eta)\,\mathrm{e}^{\mathrm{i}\kappa\xi+\sigma\tau}$ and $\delta_1 = \Delta\,\mathrm{e}^{\mathrm{i}\kappa\xi+\sigma\tau}$, etc., where σ is the growth rate of the perturbation and κ the horizontal wave number. θ, Π, and Ω denote the amplitudes of the temperature, pressure and v velocity perturbations, respectively. Δ is the amplitude of the perturbation of the interface.

Simplifying, equations (17) and (18) can be rewritten as a system of first-order ODEs:

$$\frac{\mathrm{d}X_\ell}{\mathrm{d}\eta_\ell} = F_\ell X_\ell \quad \text{(in liquid)} \tag{19}$$

$$\frac{\mathrm{d}X_{2\phi}}{\mathrm{d}\eta_{2\phi}} = F_{2\phi}X_{2\phi} \quad \text{(in two-phase)} \tag{20}$$

where

$$X_\ell = \left[\frac{\mathrm{d}\Pi}{\mathrm{d}\eta_\ell}, \frac{\mathrm{d}\Theta}{\mathrm{d}\eta_\ell}, \Pi, \Theta, \Delta\right]^{\mathrm{T}}$$

and

$$X_{2\phi} = \left[\frac{\mathrm{d}\Pi}{\mathrm{d}\eta_{2\phi}}, \Pi, S, \Delta\right]^{\mathrm{T}}$$

where the superscript T denotes a transpose.

F_ℓ is a 5×5 matrix in the liquid region defined by

$$F_\ell = \begin{bmatrix} 0 & -Ra\,\delta_0 & \kappa^2\delta_0^2 & 0 & \eta_\ell^2\kappa^2\delta_0^2\,Ra - Ra \\ -1 & 0 & 0 & -Ra\,\delta_0+\kappa^2\delta_0^2+\sigma\beta_1\delta_0^2 & -Ra\,\eta_\ell-\kappa^2\eta_\ell\delta_0-\eta_\ell\delta_0\beta_1\sigma \\ 1 & 0 & 0 & 0 & 0 \\ 0 & 1 & 0 & 0 & 0 \\ 0 & 0 & 0 & 0 & 0 \end{bmatrix}.$$

Similarly, $F_{2\phi}$ is a 4×4 matrix in the two-phase region defined by

$$F_{2\phi} = \begin{bmatrix} 0 & -\dfrac{a_3}{a_1}-\dfrac{a_2}{a_1}c_1 & -\dfrac{a_4}{a_1}-\dfrac{a_2}{a_1}c_2 & -\dfrac{a_5}{a_1}-\dfrac{a_2}{a_1}c_3 \\ 1 & 0 & 0 & 0 \\ 0 & c_1 & c_2 & c_3 \\ 0 & 0 & 0 & 0 \end{bmatrix}$$

where

$$c_1 = -\frac{b_3-b_1\dfrac{a_3}{a_1}}{b_2-b_1\dfrac{a_2}{a_1}},\quad c_2 = -\frac{b_4-b_1\dfrac{a_4}{a_1}}{b_2-b_1\dfrac{a_2}{a_1}},\quad c_3 = -\frac{b_5-b_1\dfrac{a_5}{a_1}}{b_2-b_1\dfrac{a_2}{a_1}};$$

$$a_1 = -\frac{k_{r\ell}}{(1-\delta_0)^2},\quad a_2 = -\frac{1}{(1-\delta_0)^2}\frac{\mathrm{d}p_0}{\mathrm{d}\eta_{2\phi}}+\frac{1}{1-\delta_0}Ra,\quad a_3 = k_{r\ell}\kappa^2,\quad a_4 = \phi\sigma,\quad a_5 = k_{r\ell}\frac{\eta_{2\phi}}{1-\delta_0}\kappa^2\frac{\mathrm{d}p_0}{\mathrm{d}\eta_{2\phi}};$$

$$b_1 = -\frac{k_{rv}}{(1-\delta_0)^2},\quad b_2 = \frac{1}{(1-\delta_0)^2}\frac{\mathrm{d}p_0}{\mathrm{d}\eta_{2\phi}}-\frac{1}{1-\delta_0}Ra_{2\phi},\quad b_3 = k_{rv}\kappa^2,\quad b_4 = -\phi\sigma,\quad b_5 = k_{rv}\frac{\eta_{2\phi}}{1-\delta_0}\kappa^2\frac{\mathrm{d}p_0}{\mathrm{d}\eta_{2\phi}}.$$

The **boundary conditions** are:

liquid

$$\text{at}\quad \eta_\ell = 0:\quad BC_1 X_\ell = 0$$

where

$$BC_1 = \begin{bmatrix} 0 & 0 & 1 & 0 & 0 \\ 0 & 0 & 0 & 1 & 0 \end{bmatrix};$$

two-phase

$$\text{at}\quad \eta_{2\phi} = 0:\quad BC_3 X_{2\phi} = 0$$

where

$$BC_3 = \begin{bmatrix} \dfrac{k_{r\ell}}{1-\delta_0} & 0 & \dfrac{1}{1-\delta_0}\dfrac{\mathrm{d}p_0}{\mathrm{d}\eta_{2\phi}}-Ra & \dfrac{k_{r\ell}}{(1-\delta_0)^2}\dfrac{\mathrm{d}p_0}{\mathrm{d}\eta_{2\phi}} \\ \dfrac{k_{rv}}{1-\delta_0} & 0 & -\dfrac{1}{1-\delta_0}\dfrac{\mathrm{d}p_0}{\mathrm{d}\eta_{2\phi}}+Ra_{2\phi} & \dfrac{k_{rv}}{(1-\delta_0)^2}\dfrac{\mathrm{d}p_0}{\mathrm{d}\eta_{2\phi}} \end{bmatrix}.$$

The **compatibility conditions** at the interface ($\eta_\ell = \eta_{2\phi} = 1$) can be written as

$$BC_2\begin{bmatrix} X_\ell \\ X_{2\phi} \end{bmatrix} = 0$$

where

$$BC_2 = \begin{bmatrix} 0 & 0 & 1 & 0 & 0 & 0 & -1 & 0 & 0 \\ 0 & 0 & 0 & 1 & 0 & 0 & 0 & 0 & 0 \\ -\dfrac{1}{\delta_0} & 0 & 0 & -Ra & -\dfrac{Ra}{\delta_0} & z_1 & 0 & z_2 & z_3 \\ 0 & \dfrac{1}{\delta_0} & 0 & 0 & -\dfrac{1}{(1-\delta_0)^2} & z_4 & 0 & z_5 & z_6 \\ 0 & 0 & 0 & 0 & 1 & 0 & 0 & 0 & -1 \end{bmatrix}$$

and

$$z_1 = -\left(\frac{k_{r\ell}}{1-\delta_0} + \bar{\mu}_\ell \bar{\rho}_v \frac{k_{rv}}{1-\delta_0}\right), \quad z_2 = -\left(\frac{1}{1-\delta_0}\frac{dp_0}{d\eta_{2\phi}} - Ra - \frac{\bar{\mu}_\ell \bar{\rho}_v}{1-\delta_0}\frac{dp_0}{d\eta_{2\phi}} + \bar{\mu}_\ell \bar{\rho}_v Ra_{2\phi}\right)$$

$$z_3 = -\left(\frac{k_{r\ell}}{(1-\delta_0)^2}\frac{dp_0}{d\eta_{2\phi}} + \bar{\mu}_\ell \bar{\rho}_v \frac{k_{rv}}{(1-\delta_0)^2}\frac{dp_0}{d\eta_{2\phi}} + \alpha_1 \sigma\right), \quad z_4 = \bar{\mu}_\ell \bar{\rho}_v \lambda \frac{k_{rv}}{1-\delta_0}$$

$$z_5 = \bar{\mu}_\ell \bar{\rho}_v \lambda\left(-\frac{1}{1-\delta_0}\frac{dp_0}{d\eta_{2\phi}} + Ra_{2\phi}\right), \quad z_6 = \bar{\mu}_\ell \bar{\rho}_v \lambda \frac{k_{rv}}{(1-\delta_0)^2}\frac{dp_0}{d\eta_{2\phi}} - \alpha_2 \sigma$$

where α_1 and α_2 are evaluated using the basic state saturation S_0.

The perturbation state is governed by equations (19) and (20), two boundary conditions involving BC_1 and BC_3, and the interface condition involving BC_2. The system consists of five ODEs for the liquid region, four ODEs for the two-phase region, and nine boundary/compatibility equations.

3.3. *Method of solution*

The solution of equations (19) and (20) is based on the shooting technique suggested by Davey [8]. We consider the solution vector X_ℓ and express the relation between $X_\ell = X_\ell^0$ at $\eta_\ell = 0$ and $X_\ell = X_\ell^1$ at $\eta_\ell = 1$ as

$$X_\ell^1 = B_\ell X_\ell^0$$

where B_ℓ is the transfer matrix for the liquid region. A basic assumption is that B_ℓ depends only on the eigenvalues (σ, κ) and the parameters of the problem (Ra, Q_b) and not on the boundary conditions. Similarly, we can write

$$X_{2\phi}^1 = B_{2\phi} X_{2\phi}^0$$

where $B_{2\phi}$ is the transfer matrix for the two-phase region.

For given values of $(Ra, Q_b, \sigma, \kappa)$, the ODEs given by equations (19) and (20) can be integrated from $\eta = 0$ to 1 by sequentially using for the vector X^0 (i.e. the vector representing the boundary conditions at $\eta = 0$) the orthonormal vectors given by the columns of I, the identity matrix of the same dimension. A fourth-order Runge–Kutta scheme with 50 integration steps is used to obtain the eigenfunctions $X(\eta)$. The five vectors X_ℓ^1 of values at $\eta_\ell = 1$, and the four vectors $X_{2\phi}$ of values at $\eta_{2\phi} = 1$, form the columns of B_ℓ and $B_{2\phi}$, respectively. Orthonormalization of the solution vectors during integration is not necessary since we are analyzing stability near critical conditions. The vectors formed by the columns of B_ℓ and $B_{2\phi}$ are found to be linearly independent for the range of parameters considered here. As a check, the solution technique was used to study the onset of single-phase convection in porous media for a variety of boundary conditions [10], and was found to yield very accurate results.

By combining the results of the eigenfunction integrations with the boundary/compatibility conditions, the characteristic equation for stability can be written as

$$\mathcal{F}(Ra, Q_b, \sigma, \kappa) = 0 \tag{21}$$

where

$$\mathcal{F} = \text{Det}\begin{bmatrix} BC_1 & 0 & 0 & 0 \\ B_\ell & -I & 0 & 0 \\ 0 & & BC_2 & 0 \\ 0 & 0 & -I & B_{2\phi} \\ 0 & 0 & 0 & BC_3 \end{bmatrix}.$$

A zero value for this determinant means that the homogeneous perturbation equations have a non-trivial solution. Standard techniques for non-linear equations such as Müller's method [9] can be used to find the roots of this 18×18 determinant. The overall solution procedure requires iteration on σ. With a tentative value for σ, and Ra, Q_b and κ specified, the eigenfunction integration is performed. Then, equation (21) is solved for the new value of σ and the cycle is repeated until convergence on σ is achieved. The solution procedure allows movement of the phase change interface, with appropriate heat and mass balances satisfied, and appears to work successfully for a wide range of parameters. For neutral stability analyses, σ is set to zero, and with Q_b and κ specified, an iteration is performed on Ra to determine the critical Rayleigh number. For several cases, the exchange of stabilities was validated by showing numerically that there were no complex roots of σ in the right half plane near the onset of convection [11]. Thus, unstable solutions are exponentially growing and not time oscillatory.

4. RESULTS

The solutions to the characteristic equation (equation (21)) are analyzed in the Ra–Q_b–σ–κ parameter space, where σ and κ arise from the stability analysis. The physical property parameters are evaluated using water as the working fluid, $T_0^* = 30$ C and $T_{sat}^* = 100$ C (typical of laboratory experiments), liquid and vapor properties evaluated at T_0^* and T_{sat}^*, respectively, and a porous medium consisting of glass beads or silica sand: therefore, $\phi = 0.35$, $\bar{\rho}_v = 0.6068 \times 10^{-3}$, $\bar{\mu}_r = 38.67$, $\rho_s C_s / \rho_\ell C_\ell = 0.5820$, $\gamma = 0.03663$ and $\lambda = 7.706$. These values are held fixed.

Representative ranges examined for the Ra–Q_b–κ parameters are $0 \leqslant Ra \leqslant 200$, $0.1 \leqslant Q_b \leqslant 10$, and $10^{-2} \leqslant \kappa \leqslant 10$. The major parameter is Q_b, since this essentially controls the mean height of the two-phase region. A value of $Q_b = 1$ denotes the maximum conduction heat flux across the liquid-saturated porous layer at the onset of boiling.

4.1. *Liquid-dominated two-phase regions*

We first consider the stability of liquid layers overlying liquid-dominated two-phase regions. This corresponds to the rest state solutions on the liquid-dominated branch in Fig. 2.

4.1.1. *Dependence on wave number* (κ). Figure 3 provides a representative example of how the growth rate (σ) varies with the wave number (κ). Ra is the curve parameter and $Q_b = 2$. Both short and long wavelength disturbances are stable since $\sigma < 0$. Short wavelength disturbances (large κ) are stabilized by thermal diffusion effects, whereas long wavelength disturbances (small κ) are stabilized by viscous effects. Medium wavelength disturbances are unstable at higher Rayleigh numbers, i.e. for higher permeability porous media.

Figure 4 displays the neutral stability curves ($\sigma = 0$) for various Q_b values. The critical Rayleigh number for the onset of convection, Ra_{cr}, varies with Q_b and κ. The lowest critical Rayleigh number is found by searching for the minimum value of Ra_{cr} for all values of $Q_b \geqslant 1$ and for all disturbance wavelengths. The

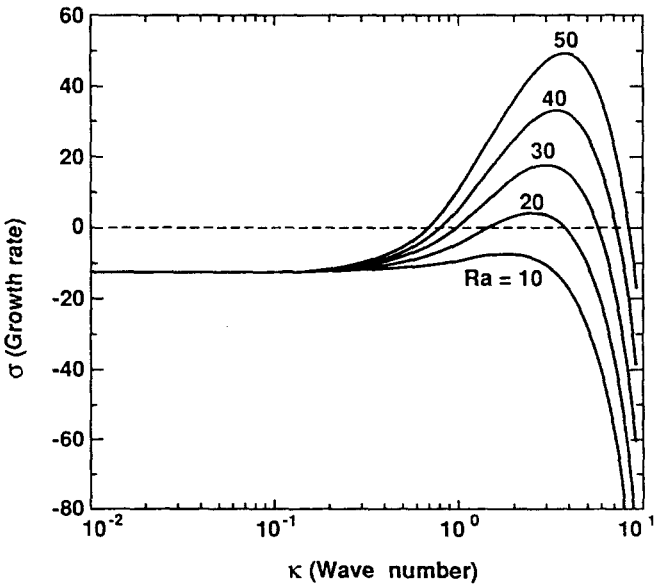

FIG. 3. Growth rate (σ) vs wave number (κ) for various Ra, with $Q_b = 2$.

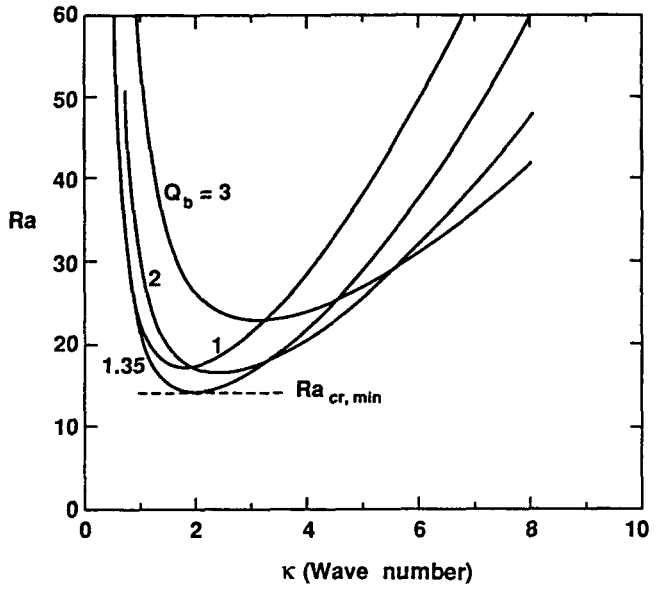

FIG. 4. Neutral stability curves for various Q_b. The minimum critical Rayleigh number for all Q_b occurs at $Q_b = 1.35$, $\kappa = 1.9$, and is $Ra_{cr,min} = 14.57$.

lowest critical Rayleigh number of the first unstable mode, $Ra_{cr,min}$, is 14.57. This occurs for $Q_b = 1.35$ and $\kappa = 1.9$. For single-phase convection, in the absence of boiling, the corresponding critical parameters are $Ra_{f,cr} = 17.7$ and $\kappa = 1.75$ for a saturated porous layer [10]. These, incidentally, correspond to the (Ra, κ) values at the minimum of the curve corresponding to $Q_b = 1$ in Fig. 4.

4.1.2. *Streamline and temperature patterns.* Illustrative streamline and isotherm patterns at neutral stability are shown in Fig. 5. The interface between the liquid and two-phase regions is indicated by the dashed lines. Base conditions are $Ra = 18.25$, $Q_b = 2$, and $\kappa = \pi$. This point lies on the neutral stability curve corresponding to $Q_b = 2$ in Fig. 4. The flow was generated by introducing a disturbance of wave number π and amplitude 0.01 at the interface, and then calculating the corresponding flow and temperature fields from equations (19) and (20). The streamlines are based on the liquid velocity ($\mathbf{v}_\ell$) in the liquid region, and the phase-averaged liquid and vapor velocity ($\mathbf{v}_\ell + \bar{\rho}_v \mathbf{v}_v$) in the two-phase region. The streamlines clearly penetrate the interface which is consistent with visualization experiments [4]. When liquid penetrates the interface, the interface distorts because it is also an isotherm. The resulting pressure gradient along the interface drives the flow in the two-phase region.

4.1.3. *Stability boundaries in Ra–Q_b space.* A comprehensive map of conductive and convective solutions in Ra–Q_b parameter space is shown in Fig. 6. The wave number is fixed at $\kappa = \pi$, a value that allows for comparison with experiments [2, 4]. The general trends in Fig. 6, however, may be expected to apply for a broad range of κ values. Four regions can be identified from linear stability theory:

(I) conductive liquid layer;
(II) convective liquid layer;
(III) conductive liquid layer above a two-phase layer;
(IV) convective liquid layer above a two-phase layer.

The onset of boiling is indicated by curve ABE. For Q_b values above this curve, boiling occurs with a liquid layer overlying a two-phase zone. The two-phase boiling zone is liquid-dominated. For Q_b values below curve ABE, boiling does not occur and the liquid phase fills the porous layer. The onset of convection in the liquid layer is denoted by curve CBD. Convection occurs to the right of the curve, and not to the left. Curve CBD thus defines the critical Rayleigh number, Ra_{cr}, as a function of Q_b for a fixed value of κ.

Curve BD in Fig. 6 is obtained from the present stability analysis. It allows for the effects of boiling and serves to separate the boiling region above the curve ABE into two parts, distinguished as to whether the liquid overlying the two-phase zone is purely conductive (III) or convective (IV). Curve BC, on the other hand, divides the non-boiling, single-phase region below curve ABE into purely conductive (I) and convective (II) parts. Curve BC thus defines the onset of single-phase convection in a horizontal porous layer. The associated critical Rayleigh number may be found with the present (or other) analysis method. For an impermeable, constant-heat-flux bottom and a permeable, isothermal top, the result is $Ra_{f,cr} = 23.17$ when $\kappa = \pi$. Curve BC therefore corresponds to $Ra_{cr} Q_b = 23.17$ after converting to the temperature-based Rayleigh number.

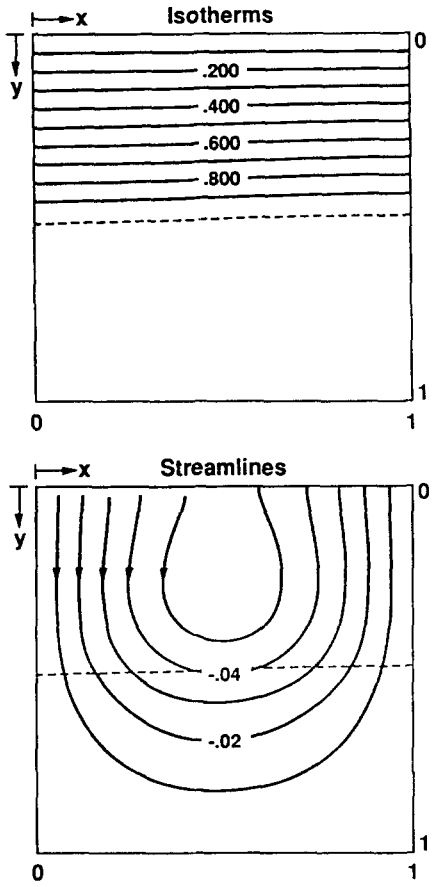

FIG. 5. Isotherms (top) and streamlines (bottom) at neutral stability for $Q_b = 2$, $\kappa = \pi$, and $Ra = 18.25$. The dotted line is the interface.

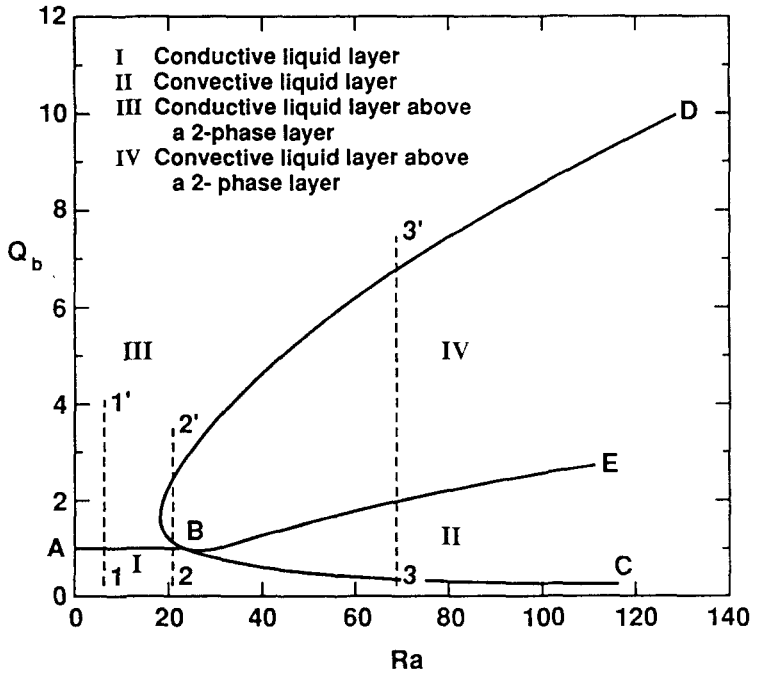

FIG. 6. Map of conductive and convective solutions in Ra–Q_b parameter space for liquid-dominated two-phase systems ($\kappa = \pi$).

In laboratory experiments, boiling occurs when the temperature at the bottom reaches the saturation temperature (T^*_{sat}). The branch AB of curve ABE in Fig. 6 corresponds to $Q_b = 1$, and represents the onset of boiling before the onset of convection. Along AB, there exists a liquid-filled porous layer with a bottom temperature at T^*_{sat}. The branch BE represents the onset of boiling after convection already exists within a liquid-filled porous layer. Since the convective amplitude is finite, curve BE cannot be obtained using the present analysis. Instead, curve BE was obtained from numerical solutions of the single-phase convection problem. Ra–Q_b values were noted when the bottom temperature reached T^*_{sat}. Further details are available in ref. [11].

The comprehensive map in Fig. 6 is extremely useful for interpreting boiling experiments in the laboratory. In particular, the map reveals that a complex range of behaviors may exist in the vicinity of point B when simple process paths are followed in Ra–Q_b space. Experiments conducted on a porous medium with constant properties by varying the bottom heat flux are an example. Such process paths are represented by vertical dashed lines in Fig. 6. We might imagine three experimental scenarios. At low Ra (as indicated by line 1–1′), the liquid region is conductive before and after the onset of boiling. This is consistent with the experiments of ref. [1] on low-permeability porous beds ($K = 11 \times 10^{-12}$ m^2). At higher Ra (as indicated by line 2–2′), the liquid region is conductive before the onset of boiling, but becomes convective almost immediately when boiling starts, which agrees with the observations of Sondergeld and Turcotte [2] ($K = 70 \times 10^{-12}$ m^2). For large Ra (as indicated by line 3–3′), the liquid region becomes convective before the onset of boiling and stays convective after the onset of boiling, which is consistent with the experiments of ref. [3] on high permeability porous beds ($K = 1600 \times 10^{-12}$ m^2). In addition, Bau and Torrance [3] observed that at large heat fluxes, the liquid region reverts back to a conductive state which again is consistent with Fig. 6. More quantitative comparisons with experiments are not possible because of side wall heat losses and large uncertainties in the properties of the porous medium. The qualitative agreement is strong, however, and the map provides an interpretation of previously unexplained experimental observations.

4.2. *Vapor-dominated two-phase regions*

We next consider the stability of liquid layers overlying vapor-dominated two-phase regions. This corresponds to the rest-state solutions on the vapor-dominated branch in Fig. 2. Since the density difference between the liquid and two-phase regions is greater when the rest-state saturation in the two-phase region lies on the vapor-dominated branch of Fig. 2 rather than the liquid-dominated branch, we expect gravitational instability to be the dominant instability mechanism. To show that this is in fact true, we consider the special case when buoyancy effects in the liquid region are negligible, i.e. $\beta_\ell(T^*_{sat} - T^*_0) \approx 0$. This implies that $Ra = \gamma = 0$. Note, however, that $Ra_{2\phi}$ is finite, and therefore is the appropriate parameter to study this mode of instability. We carry out the stability analysis in the $Ra_{2\phi}$–Q_b–σ–κ parameter space.

The stability analysis reveals that the rest state is unstable for large values of $Ra_{2\phi}$ and a range of Q_b values. Only long wavelength disturbances are stable, while both short and medium wavelength disturbances are unstable. This is because thermal diffusion effects, which typically stabilize short wavelength disturbances, are unimportant when thermal buoyancy is neglected. The main stabilizing effect to gravitational instability is due to the phase change processes at the interface [6].

The neutral stability curve ($\sigma = 0$) for a fixed wave number ($\kappa = \pi$) in $Ra_{2\phi}$–Q_b space is shown in Fig. 7. The critical value of $Ra_{2\phi}$, $Ra_{2\phi,cr}$, varies with Q_b and κ. For $\kappa = \pi$, the minimum value of $Ra_{2\phi,cr}$ is 18.95, occurring for $Q_b = 1.4$. With water as a working fluid, and the bed parameters referred to at the start of this section and $H = 0.2$ m, the minimum value of $Ra_{2\phi,cr}$ in Fig. 7 implies a bed permeability of $K = 1.6 \times 10^{-12}$ m^2. Thus, a one-dimensional vapor-dominated system will be stable only for permeabilities lower than this value. However, when the stability analysis in $Ra_{2\phi}$–Q_b–σ–κ space is repeated for rest-state solutions on the liquid-dominated branch of Fig. 2, it is found that a one-dimensional liquid-dominated system is unconditionally stable when buoyancy effects are negligible ($Ra = \gamma = 0$).

To illustrate that the usefulness of the present analysis is not restricted to laboratory-scale porous media, we consider the vapor-dominated geothermal system studied by Schubert and Straus [6]. The physical property parameters for this porous medium are $\phi = 0.05$, $\bar{\rho}_v = 0.2075$, $\bar{\mu}_\ell = 8.176$, $\rho_s C_s / \rho_\ell C_\ell = 0.6475$ and $\lambda = 1.757$. In addition, $H = 1000$ m, $T^*_{sat} = 242$°C and $T^*_0 = 20$°C. Consistent with the assumptions of Schubert and Straus, we neglect buoyancy effects, i.e. $\gamma = 0$ and $Ra = 0$. Carrying out the stability analysis in $Ra_{2\phi}$–Q_b space, assuming $\kappa = \pi$ and $\sigma = 0$, we find that the minimum value of $Ra_{2\phi,cr}$ is 2.56, occurring for $Q_b = 1.2$. This corresponds to a critical bed permeability of 51×10^{-18} m^2, which compares well with the reported value of 40×10^{-18} m^2. It should be pointed out that while the present analysis assumes a two-phase region underlying the liquid region, Schubert and Straus assumed a dry vapor region underlying the liquid region.

4.3. *Stability of rest state solutions*

Based on the analysis in the two foregoing subsections, we now address the stability of the rest-state two-phase solutions given in Fig. 2. For the present discussion, we assume that the wave number κ is fixed at π. However, the inferences drawn here may be expected to apply over a wide range of κ.

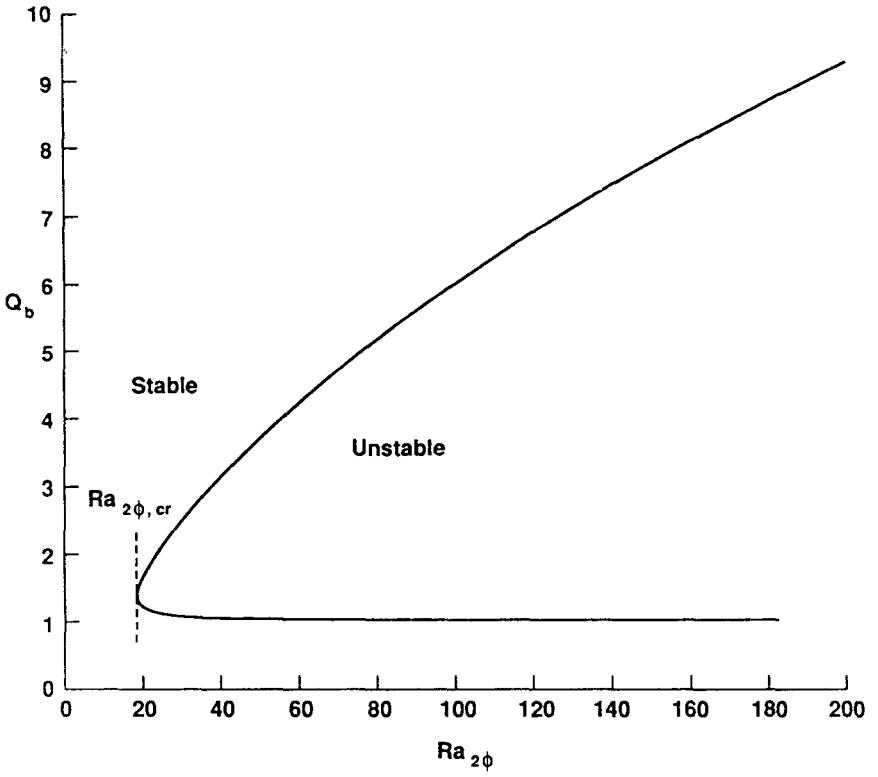

FIG. 7. Neutral stability curve for vapor-dominated systems ($Ra = 0$, $\kappa = \pi$).

The stable region on the liquid-dominated branch of Fig. 2 can be deduced from curve BD in Fig. 6. The minimum value of liquid saturation corresponding to the rest-state solution (S_0) on curve BD is ≈ 0.98. Liquid-dominated rest-state solutions with S_0 lower than this value are stable, while those with S_0 higher than this value are unstable. The instability in such liquid-dominated systems is driven by buoyancy in the overlying liquid region. It should be pointed out that while stability of the liquid-dominated rest-state solutions at large Q_b (low S_0) is indicated by the linear stability theory (Fig. 6), a numerical solution of the complete equations [11] has suggested that instability may be possible provided the perturbations are large enough so that second-order effects become important. The numerical solution of the complete equations in Ra–Q_b parameter space will be the subject of a forthcoming article.

Similarly the stable regions on the vapor-dominated branch of Fig. 2 can be inferred from Fig. 7. The maximum value of S_0 on the curve in Fig. 7 is ≈ 0.02, which corresponds to an ordinate value, $Q_b/(\lambda(Ra_{2\phi} - Ra)\bar{\rho}_v\bar{\mu}_v)$, of 0.46 in Fig. 2. Vapor-dominated rest-state solutions below the (0.02, 0.46) point in Fig. 2 are unstable, while those above this point are stable. The mechanism for this instability is clearly gravitational because the buoyancy driven instability is observed only for larger values of S_0 (>0.98).

5. SUMMARY

The stability of boiling in fluid-saturated horizontal porous layers heated from below and cooled from above is analyzed. The basic state is one-dimensional consisting of a liquid region overlying an isothermal two-phase region. Conditions for the onset of convection in the liquid region are investigated. Both liquid- and vapor-dominated two-phase regions are considered. For liquid-dominated systems, the convective instability is mainly driven by buoyancy in the liquid region, and the results of the stability analysis agree well with previous experimental studies. For vapor-dominated systems, the instability is mainly driven by the density difference between the liquid and two-phase regions.

Acknowledgements—The authors would like to thank Dr Mihir Sen for many helpful discussions. This work has been supported by the Division of Mechanical Engineering and Applied Mechanics of the National Science Foundation under Grant MEA-8401489. Computations were carried out using the Cornell National Supercomputer Facility, a resource of the Center for Theory and Simulation in Science and Engineering (Cornell Theory Center), which receives major funding from the National Science Foundation and IBM Corporation, in addition to support from New York State and members of the Corporate Research Institute.

REFERENCES

1. H. H. Bau and K. E. Torrance, Boiling in low-permeability porous materials, *Int. J. Heat Mass Transfer* **25**, 45–55 (1982).
2. C. H. Sondergeld and D. L. Turcotte, An experimental study of two-phase convection in a porous medium with applications to geological problems, *J. Geophys. Res.* **82**, 2045–2053 (1977).
3. H. H. Bau and K. E. Torrance, Thermal convection and boiling in a porous medium, *Lett. Heat Mass Transfer* **9**, 431–441 (1982).
4. C. H. Sondergeld and D. L. Turcotte, Flow visualization studies of two-phase thermal convection in a porous layer, *Pure Appl. Geophys.* **117**, 321–330 (1978).
5. C. S. Yih, *Fluid Mechanics*, Chap. 9. West River Press, Ann Arbor, Michigan (1979).
6. G. Schubert and J. M. Straus, Gravitational stability of water over steam in vapor-dominated geothermal systems, *J. Geophys. Res.* **85**, 6505–6512 (1980).
7. K. E. Torrance, Boiling in porous media. *ASME/JSME Thermal Engng Joint Conf. Proc.*, Vol. 2, pp. 593–606 (1983).
8. A. Davey, A simple numerical method for solving Orr–Sommerfeld problems, *Q. J. Mech. Appl. Math.* **26**, 401–411 (1973).
9. S. D. Conte and C. de Boor, *Elementary Numerical Analysis: an Algorithmic Approach*, Chap. 2. McGraw-Hill, New York (1972).
10. R. J. Ribando and K. E. Torrance, Natural convection in a porous medium: effects of confinement, variable permeability and thermal boundary conditions, *J. Heat Transfer* **98**, 42–48 (1976).
11. P. S. Ramesh, Boiling and natural convection in a fluid-saturated porous medium, Ph.D. thesis, Cornell University, Ithaca, New York (1988).

STABILITE DE L'EBULLITION DANS DES MILIEUX POREUX

Résumé—On étudie l'apparition de la convection en rouleaux bidimensionnels en présence d'ébullition pour une couche poreuse horizontale saturée en fluide. La couche est chauffée par le bas et refroidie par le haut. La structure au repos consiste en une région liquide surmontant une région diphasique. Les deux paramètres importants du problème sont le nombre de Rayleigh dans la région liquide (Ra) et le flux thermique adimensionnel à la base (Q_b). On étudie les régions diphasiques l'une dominée par le liquide et l'autre par la vapeur. Pour les systèmes dominés par le liquide, l'instabilité de convection est pilotée principalement par le flottement dans la région liquide, tandis que pour les systèmes dominés par la vapeur, l'instabilité est conduite par l'instabilité gravitationnelle des couches supérieures. Pour les systèmes dominés par le liquide, un diagramme de stabilité Ra–Q_b est utilisé pour interpréter les expériences principales en laboratoire.

ZUR STABILITÄT DES SIEDENS IN PORÖSEN MEDIEN

Zusammenfassung—Es wird das Einsetzen der Konvektion in Form zweidimensionaler Walzen in einer flüssigkeitsgesättigten horizontalen porösen Schicht in Anwesenheit von Sieden untersucht. Die Schicht wird von unten beheizt und von oben gekühlt. Die Phasenstruktur im Ruhezustand besteht aus einem Flüssigkeitsgebiet, dem ein Zweiphasengebiet überlagert ist. Zwei wesentliche Parameter sind die Rayleigh-Zahl im Flüssigkeitsgebiet (Ra) und die dimensionslose Wärmestromdichte an der unteren Berandung (Q_b). Es wird sowohl das flüssigkeitsbestimmte als auch das dampfbestimmte Zweiphasengebiet betrachtet. Für flüssigkeitsbestimmte Systeme wird die Konvektionsinstabilität hauptsächlich durch Auftriebskräfte in der Flüssigkeit bewirkt, während für dampfbestimmte Systeme die Instabilität durch die Schwerkraftinstabilität der darüberliegenden Schichten bestimmt wird. Es wird ein Stabilitätsdiagramm in der Ra–Q_b-Ebene für flüssigkeitsbestimmte Systeme verwendet, um frühere Laborexperimente zu interpretieren.

УСТОЙЧИВОСТЬ КИПЕНИЯ В ПОРИСТЫХ СРЕДАХ

Аннотация—Исследуется возникновение двумерных конвективных валов при кипении в насыщенном жидкостью горизонтальном пористом слое. Слой нагревается снизу и охлаждается сверху. Он состоит из области, заполненной жидкостью, и из расположенной под ней двухфазной области. Основными параметрами данной задачи являются число Рэлея в жидкой области Ra и безразмерный тепловой поток у нижней границы Q_b. Исследуются двухфазные области с преобладанием как жидкости, так и пара. В системах с преобладанием жидкой фазы неустойчивость конвекции обусловлена преимущественно подъемной силой в области, заполненной жидкостью, в то время как в системах с преобладанием пара она вызвана гравитационной нестабильностью вышележащих слоев. Для интерпретации предыдущих лабораторных экспериментов в случае систем с преобладанием жидкости используется схема устойчивости в пространстве параметров Ra–Q_b.